Republic of Iraq
Ministry of Higher Education and
Scientific Research
University of Diyala
College of Science
Department of Physics

Preparation and characterization of CuO-Ag nanocomposites using plasma jet method for gas sensor

A thesis

Submitted to the College of Science University of Diyala, in Partial Fulfillment of the Requirements for the Degree of Master in Physics

Shaimaa Fadhil Mohamad

B. Sc. in Physics-University of Baghdad (2002)

Supervised By

Assist. Prof. Dr
Rudainah Ali Lateef

Assist. Prof. Dr.
Olfat Ahmad Mahmood

2025 A.D.

1446 A.H.

((ويَسْأَلُونَكَ عَنِ الرُّوحِ قُلِ الرُّوحُ مِنْ
أَمْرِ رَبِّي وَمَا أُوتِيتُم مِّنَ الْعِلْمِ إِلَّا قَلِيلًا))

صدق الله العلي العظيم

سورة الاسراء –

الآية ٨٥

Abstract

This study successfully made pure copper oxide nanoparticles (Cuo NPs), pure silver nanoparticles (Ag NPs), and copper oxide composites with silver (CuO-Ag NPs) at different weight ratios (0, 1, 3, 6, 9 and 12 wt. %) using the plasma jet preparation method. A simple, cheap, and safe method called plasma jet technique was used to make pure and highly solid CuO NPs, Ag NPs, and CuO/Ag NPs. We looked at the structure (FESEM, EDX, XRD, and FT-IR), optical properties, and gas sensing performance of synthesized CuO NPs and Ag NPs samples. We also looked at how the doping ratio affects the properties of the CuO NPs thin films.

The field emission scanning electron microscopy (FESEM) and X-ray diffraction (XRD) results showed that particles were highly crystalline and pure, with a cubic-CuO NPs structure that looked like a semi-spherical shape and a monoclinic Ag NPs structure that looked like a uniform spherical Ag NPs shape. The average particle size was 50 nm for the FESEM particles and 38 nm for XRD particles. Both EDX and FTIR tests showed that the Cu NPs and Ag NPs worked well together as dopants in the CuO/Ag nanocomposite films. They also showed the chemical makeup, functional groups, and interactions between the two.

The absorbance and transmittance spectra were examined within the wavelength range of 300–1100 nm. The results indicated that the pure CuO solution exhibited a higher absorption capability at a specific wavelength, while the addition of Ag NPs resulted in a decrease in absorbance capability. The transmittance exhibited an inverse relationship with the wavelength. Furthermore, the absorbance and transmittance values are considerably influenced by the Ag NPs content and wavelength. It was observed that the addition of varying Ag NPs contents to a purified CuO NPs solution resulted in a decrease in transmittance and an increase in absorption.

In contrast, the reflectance results indicated that the refractive index decreased as the wavelength increased, which was a consequence of the addition of Ag NPs. The purified CuO NPs solution, on the other hand, obtained the highest values of reflectance. The absorption coefficient of pure CuO NPs solution exhibited a high peak in the energy range of (3 – 3.5 eV) as a function of photon energy. However, the absorption coefficient value experienced a significant decrease as the Ag NPs within the CuO solution structure increased.

The energy band gaps of the prepared solutions were calculated. The resulting solutions exhibited a direct energy band gap. It was found that the energy band gap decreases at low silver nanoparticle ratios but increases at high ratios. The addition of silver nanoparticles likely changes the energy gap due to the increased occurrence of impurities that affect the band gap structure. The solution of copper oxide nanoparticles doped at a ratio of (0.01) showed the lowest energy band gap value (2.513 eV), while the highest energy gap value was at a ratio of (0.12) equal to (3.185 eV). The electronic transitions of the prepared films are direct.

The results also indicated that the refractive index and extinction coefficient of clean and doped samples decrease as the photon energy increases. The real dielectric constant increased as the concentration of Ag NPs in pure CuO NPs varied. Conversely, the imaginary dielectric constant decreased linearly as the incident photon energy decreased in pure materials. However, the rate of rise changed when Ag NPs were added.

The electrical resistance (Ra) of all thin film sensors is stable in air, as demonstrated by the gas sensor characterizations. However, the electrical resistance (Rg) of (A) sensor increased as a function of exposure time when the thin film sensors were tested under NO2 gas (500 ppm). In the opened gas case, the (Rg) of (B to G) sensors decreased, while the (Rg) of (A) sensor decreased and then swiftly increased in the closed gas case. The electrical resistance increased and the electrical conductivity of all prepared sensors decreased when

NO_2 gas was administered, resulting in n-type behavior. NO_2 gas was present in all n-type sensors; however, the reverse behavior occurred when NO_2 was applied to B-G thin film sensors with P-type behaviors.

The sensitivity (S %) of the prepared sensors to NO_2 gas revealed varying values in relation to the doping content and temperature. In general, all of the sensors exhibited adequate sensitivity (S %) at moderate temperatures (50, 100, and 150 °C) and low sensitivity at high temperatures (200 °C). However, the addition of Ag NPs resulted in a substantial increase in the sensitivity values. In contrast, the sensitivity (S %) is reduced as a result of the increased resistance of all sensors (Rgas > Rair) during NO_2 exposure in the closed gas chamber.

At temperatures of 100 °C, the B sensor exhibited the highest response time of (51.12 seconds) and the highest recovery time of (56.763 seconds), whereas the F sensor exhibited the lowest response time and recovery time of (1.17 seconds) and (19.62 seconds) at temperatures of 50 °C and 200 °C, respectively. The performance characteristics of the sensors that are obtained in response to NO_2 gas are significantly influenced by the exposure temperature.

Chapter One

Introduction and Literature review

(1.1) Introduction

Nanoparticles are defined as materials that are smaller than 100 nm in size and can be handled and studied as a whole. Measurements of length and diameter can be used as effective screening criteria. The two basic types are “compressed materials” and “nanoembolics”. The sensory and scientific fields are particularly interested in the potential of nanoparticles [1].

(1.2) Nanomaterials

The definition of nanocomposites has been considerably broadened to encompass a wide range of systems, including amorphous, one-dimensional, two-dimensional, and three-dimensional materials, which are composed of distinct components that are amalgamated at the nanometer scale. It can benefit from impact and abrasion resistance, as well as being lightweight. Additionally, it exhibits high-temperature resistance performance characteristics. The advantages of nanocomposites over conventional compounds are not limited to their strength. Some nanocomposites are also suitable for use as insulators and wire coatings due to their low flammability, resistance, and high temperature. Nanomaterials are frequently combined with bulk metal oxide nanomaterials to enhance their properties, as they possess exceptional qualities [2]. Nanocomposites are materials that are reinforced with nanoparticles, as their name suggests.

So, compound materials can be defined as systems in which two or more substances participate that are not capable of dissolution and complete interaction between them, that is, they do not lead to the formation of a new chemical substance, as each substance represents a separate phase in the system, that is, the formation of a new substance with physical properties that are different from the properties of its components included in its composition, where They are more suitable for industrial applications.

(1.3) Classifications of Nanomaterials

According to their dimensions, nanostructures are classified. [3] Figure 1.1 illustrates a variety of nanomaterials that are categorized according to their dimensions.

- Nanomaterials that are zero-dimensional (0D) are defined as having dimensions in the nanometer range in all three spatial orientations. Metal nanoparticles and quantum dots are examples of these.

- One-dimensional, or quasi-one-dimensional, nanomaterials are characterized by their length, which extends beyond one nanometer. Examples of these materials include nano-tubes and nano-rods.

- Two-dimensional (2D) nanomaterials are characterized by having two dimensions within the nanometer scale. This category includes structures such as nano-layers and nanosheets.

- Three-dimensional (3D) nanomaterials are materials that possess overall dimensions within the millimeter or micron range but feature nanoscale characteristics at larger distances. These materials are designed to be used as structures on a nanoscale [4].

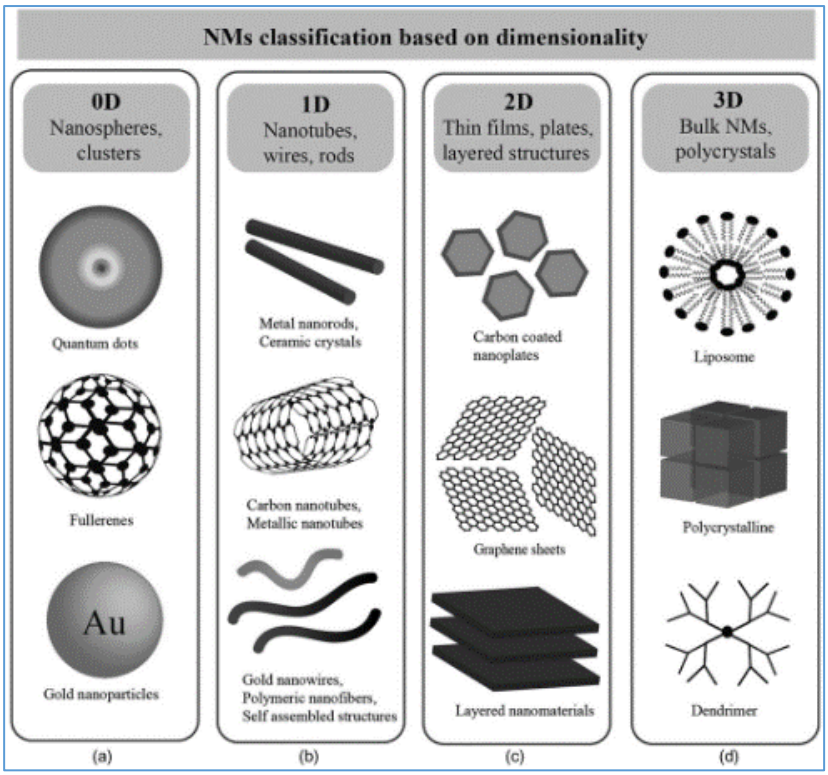

Figure 1.1: Nanoparticles includes four states depend on dim.: (a) 0-D, (b) 1-D, (c) 2-D, and (d) 3-D [4].

(1.4) Nanoparticles Synthesis

Nanoparticles can be produced through a variety of methods, such as physical, chemical, and biological methods. The following is a comprehensive description of each of these techniques:

(1.4.1) Chemical Methods

The creation for nanomaterials is facilitated by a decrease the metallic ions at appropriate circumstances through the synthetic chemical method. Here are some of the chemistry techniques:

• A chemical reducing approach provides a generally accepted and straightforward approach for producing nanoparticles of metal. This process involves producing nanoparticles through reducing metals constituent

components with a suitable reducing agent at room temperature or above. Sodium borohydride, hexamethylenetetramine, and sodium citrate are some of the most often used reducing agents in this technique. Stabilization agents like sodium lauryl sulfate and polyvinylpyrrolidone are often employed to keep small particles without swarming to the mixture [5, 6].

Emulsions are clear combinations of oil, water, and surfactant. Micro-emulsion enhances processes in the tiny particles production procedure via the combination of soluble in oil reducers with a water-soluble predecessors [7].

1. This process generates nanoparticles at high temperatures from water and components which cannot generally dissolve in water. Chemical solvothermal method, which is similar to the hydrothermal approach, uses a solvent instead of water, and the reactions take place under supercritical conditions [8].
2. The Sonic chemical-based approach produces nanoparticles of metal via subjecting a precursor solution to ultrasonic radiation at frequencies that range from 20 kHz to 10 MHz. Cavitation, also occurs, resulting in the production of nanomaterials. The process described above is regarded as one of the most straightforward to create nanomaterials [4].
3. The method of creating inorganic materials using sol-gel technology involves first creating a sol, or colloidal suspension, which is then gelled to create a two-phase system with a liquid phase and a solid phase. Nanocoatings are frequently applied to textiles using this technique. Sol-gel nanoparticles are usually synthesized using metal alkoxides [3]. These metal alkoxides react with water during the sol-gel process, hydrolyzing and condensing in the presence of a catalyst, which might be a base or a mineral acid [5, 7].

(1.4.2) Biological Methods

It has been shown that producing nanoparticles chemically is both affordable and environmentally beneficial. As a result, several scientists have proposed

commercial and ecologically beneficial ways to synthesize nanoparticles. These days, a variety of plant extracts and microbes are employed in place of artificial stabilizers and insecticides [9].

(1.4.3) Physical Methods

This method uses both condensation and evaporation procedures in a heated tube at air pressure to produce nanoparticles. After being transformed to vapor, the initial material is transported by a gas into a furnace, where it condenses to create nanomaterials.

1. Physical Vapor Deposition (PVD)

In PVD, vaporized material is physically transferred to a solid substrate, where it condenses. Techniques like sputtering and heat evaporation are part of this approach. This includes creating thin metal films for electrical applications, such as those made of gold or silver [10].

2. Laser Ablation

This method involves the use of laser beams that are focused to remove material from a solid target. The ejected material condenses to form nanoparticles in a gas or solution, as demonstrated in the synthesis of metal oxide nanoparticles using laser ablation in liquids [11].

3. Solvothermal and Hydrothermal Methods

These methods employ high-temperature and high-pressure conditions to dissolve precursors in a solvent, thereby enabling the formation of nanoparticles. For example, the synthesis of titanium dioxide nanoparticles using a solvothermal process [12].

4. Mechanical Milling

Mechanical forces are employed to produce nanoparticles by pulverizing bulk materials in this method. Like Synthesis of silicon nanoparticles using high-energy ball milling [13].

5. Thermal Decomposition

This technique involves the breakdown of precursors under high temperatures to produce nanoparticles like synthesis of metal sulfide nanoparticles through thermal decomposition of their corresponding metal-organic precursors [14].

6. Arc Discharge Method

Is a prominent technique used for synthesizing nanomaterials, particularly carbon nanotubes and other nanostructures, An electric discharge is produced between two electrodes in this method.

typically made of carbon or other materials. When the arc is struck, high temperatures are produced, which vaporizes the material. Upon cooling, the vapor condenses into nanoparticles or nanotubes [15].

1.5 Plasma Method

Is one of the physical methods for manufacturing nanomaterials, plasma technologies are widely used to produce different nanostructures due to their versatility and ability to produce high purity materials, plasma manufacturing methods use an ionized gas (plasma) to produce nanomaterials. The process can vary, but typically involves generating a plasma state where the temperature and energy levels are controlled to facilitate the nucleation and growth of nanoparticles. Plasma has the following advantages [16]:

-High purity and uniformity of the produced nanomaterials.

-Ability to control particle size, shape and composition by adjusting the plasma parameters.

- A wide range of materials can be produced, including metals, oxides and carbides.

Plasma represents a neutral and charged ionized gas. By definition, plasmas are quasi-neutral and conductive. This means that all positive charges are equal to all negative charges and that electrons accumulate at natural frequency due to the long-term effect of the Coulomb force. Thus, Maxwell's equations and the laws of conservation of energy and energy govern plasma particle physics. Other problems such as the presence of dust, increased magnetism and potential chemicals complicate plasma. Plasmas occur in holes and man-made reactors. Moreover, they operate in a completely different way. To better understand what the above plasma means, two points need to be considered [17]:

(1.5.1) the behavior of Collective

Magnetic fields and Coulomb interactions are among the long-range forces that affect plasmas. When plasma molecular interacts with conventional air, it maintains an electrically neutral state meaning there is no overall electromagnetic force acting on it, and its gravitational effects are minimal. Molecules generally continue their path smoothly until they bump into other molecules, and these collisions influence their movement. In plasmas, which are made up of charged particles, the dynamics of motion are quite different. As these charges move, they create regions of negative or positive charge that generate electricity. The energy of the charge also creates an electric current and a magnetic field. Therefore, other distance costs are also affected by these fields [18].

(1.5.2) Quasi-The neutrality

The equal density of positive and negative results in the formation of negative electricity in the blood. To achieve neutrality, the voltage in each part of the plasma must be negative from the limit of the blood. In other words, the

potential of each particle must be adequately protected by the population of particles around it [19].

(1.5.3) the Plasma Criteria

Know that all plasmas are ionized gases, but not all ionized gases are plasmas. In order for ionized gas to form plasma, the following conditions must be met:

1-The dimension of system (L) surely significantly larger from "Debye Length" (λ_D) is shielding distance called thickness of the sheath (λ_D « L).

2-In the "Debye sphere" the number of particles (N_D) Must be far greater than one (N_D» 1).

3- "The plasma oscillation frequency (ω) and the average time between collisions with neutral atoms (τ) must satisfy the condition ωτ > 1. This indicates that collisions play a crucial role in the behavior and regulation of the plasma." [18].

(1.6) the Parameters of Plasma

Parameter knowledge is greatly importance for improving plasma processing because those parameters are directly related to the physical and chemical impacts that occur during the plasma generation process. Plasmas are characterized by the same fundamental properties regardless of the system to which they are connected. These criteria might be classified as internal (plasma characteristics) or external (qualities of the operating control parameters). The main internal parameters of interest are [18]:

• Plasma temperature is the average temperature for each type. Typically measured in unit eV, where (l eV≈11600 K) .

• Plasma density, the number of activated species in plasma, and measured in particles per cubic meter.

• Plasma frequency (ω_{pe}), Is the frequency at which electrons in the absence of a magnetic field oscillate about their equilibrium locations.

• (λ_D) Debye length , It is the distance at which the electric field of a single charge is blocked due to the redistribution of charged particles (i, e).

(1.6.1) Determination Plasma Frequency

The plasma frequency includes the electron and ion plasma frequencies, the plasma frequency of electron (ω_{pe}) which can be written as [20]:

$$\omega_{pe} = \sqrt{\frac{e^2 n_e}{\epsilon_0 m_e}} \qquad (1.1)$$

Where e is the charge of an electron, and ε_0 is the permittivity (8.85 x 10^{-12} F/m), also m_e is the mass of an electron (9.1 x10^{-31}) .

Simplifying the equation (1.2) can be written as [21]:

$$\omega_{pe}(HZ) = 8.98\sqrt{n_e} \qquad (1.2)$$

While the ion plasma frequency (ω_{pi}) can be written as [20]:

$$\omega_{pi} = \sqrt{\mu}\ \omega_{pe} \qquad (1.3)$$

Where μ *is the ratio of electron and ion masses over charges* $\mu = m_e/m_i$, the ions oscillate much more slowly by a factor $(\frac{m_e}{m_i})^{1/2}$about the centre of mass. The collision frequency of electrons is approximately 40 times greater than that of ions as a result of the mass disparity between the two. Compared to electrons, ions exhibit a substantially lower collision frequency due to their decreased thermal velocity. This discrepancy in thermal velocity, which is proportional to the square root of the mass ratio of electrons to ions, results in

ions colliding with each other less frequently than electrons do [22]. Despite this, the electron plasma frequency is crucial because electrons are much more mobile, given that the mass ratio of protons to electrons is around 1.8×10^3. [23].

(1.6.2) Determination Debye lengths

Consequently, the applied electrical potential will develop primarily in the vicinity of the surfaces, over a distanceλ_D, which is referred to as the Debye length, as defined by [24]:

$$\lambda_D = \left(\frac{\epsilon_0 K_B T_e}{n_e e^2}\right)^{\frac{1}{2}} \quad (1.4)$$

Where n_e is the density of the electrons (m^{-3}), ε_o is the Permittivity of free space .By simplifying the equation (2.4), can be written as [25].

$$\lambda_D(cm) = 6.9\,(\frac{T_e}{n_e})^{\frac{1}{2}} \quad (1.5)$$

T_e: $Electron\ temperature$

(1.7) the Plasma Classifications

Plasma can be divided into several types. It can be classified according to power, temperature, pressure, installation and output mode. According to plasma power, it is divided into DC, AC, radio frequency and microwave. According to temperature, plasma can be classified as hot plasma and cold plasma. According to pressure, plasma can be divided into two groups: vacuum and atmospheric pressure. According to its structure, it can be divided into ring plate type, z-shaped compression type, dielectric barrier discharge type (DBD), parallel plate type, micro-cavity cathode discharge type (MHCD), etc. Plasma can be categorized based on its discharge type, including Townsend discharge, corona discharge, glow discharge, arc discharge, and streamer discharge, among others. Factors such as the pace of the electrons and the plasma's temperature influence the

energy within the plasma, which is contingent upon the nature of the energy source and the quantity of electricity delivered [26].

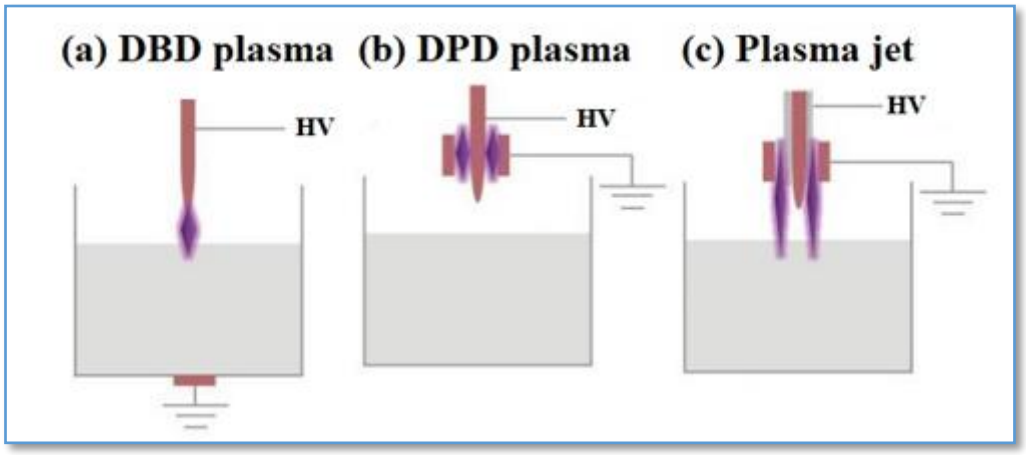

Figure 1.2: Types of water phase to gas phase discharge: (a) plasma DBD in contact with surface water, (b) plasma DBD not in contact with surface water, and (c) plasma jet water in contact with water [27].

(1.7.1) Plasma Jet method

The plasma jet is a refined form of the DBD, intended to enable remote sample treatment and extend the plasma plume farther from the discharge location. Furthermore, there are no problems at the operation site because plasma jets can influence objects from a distance. Furthermore, cold plasma has a promising future in the treatment of tissues, cells, and heat-sensitive materials that need low gas temperatures. Figure (1.3) shows an example of a plasma jet diagram, which consists of a ground electrode and a high-voltage needle electrode. Inert gas flow, such as argon, helium, etc., is maintained by the needle electrode to aid in the breakdown process. A gas flow that creates an afterglow in the surrounding air blasts plasma into the open space from inside the needle between the electrodes. Afterglow often exhibits low temperature and various types of organisms such as excited atoms and molecules, free radicals, radiation, metastable state and ultraviolet radiation. Unwanted effects on the generated

plasma can be avoided by plasma jets .Because the active region of discharge and the afterglow region are separated spatially, it promotes high-form plasma stability near the upstream electrodes. The plasma components, including short reactive species, are carried into a far-off zone several centimetres from the discharge location due to the high gas flow rate. It is possible to synthesise and change the surface of nanomaterials by using the near-room temperature plasma in the remote location [28]. A wide range of plasma jets have been developed in the last ten years to generate plasmas with different configurations and operating characteristics. The majority of the working gases are made up of a mixture of molecular gases like Ar, H_2O, N_2, O_2, and air, as well as noble gases like argon and helium. Several types of energy, including DC, AC, RF, microwave, and pulsed voltage, are used to power plasma jets. Every plasma jet is different . Features and, given its specific constraints (configuration, power, and gas), can be used in a variety of applications. The development, understanding, and optimization of plasma jets through a variety of experimental procedures and experimental methodologies, known as plasma diagnostics, have advanced significantly. [29] Numerous diagnostic techniques have been developed and employed up to this point to characterize plasma jets. These include absorption spectroscopy, optical emission spectroscopy, probe measurements, enhanced charged-coupled device imaging techniques, mass spectrometry, Laser-induced fluorescence measurement, acoustic diagnosis, cavity ring-down spectroscopy, etc. Due to their wide range of properties, plasma jets are widely studied for various applications. Applications include food treatment, cell therapy, film deposition, surface modification, sterilisation, surface cleaning, pollution control, and the medical field. Research into plasma jets and related technologies is encouraged by these practical uses as well as the bright industrial future.

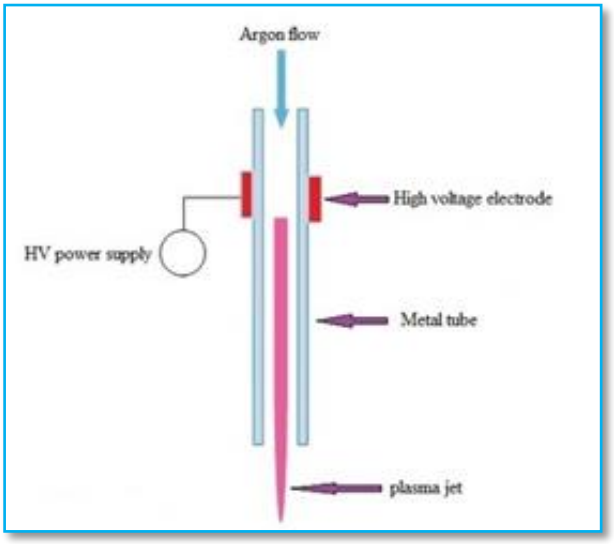

Figure 1.3: Schematic diagram of the plasma jet [30].

(1.7.2) According to temperature plasma Classification

According to the temperature of electrons, ions and neutrons, plasma can be divided into different types according to temperature and temperature. Plasmas are divided into thermal equilibrium plasmas, local thermal equilibrium plasmas, non-thermal equilibrium plasmas or non-thermal plasmas (non-equilibrium plasma) [31].

(1.7.2.1) the Plasma Thermal Equilibrium

In a plasma that is in thermal equilibrium, the temperatures of electrons (T_e), ions (T_i), and neutrals (T_n) are all equal. This common temperature typically ranges between 0.1 and 10 keV.

In high-temperature, high-density plasmas, thermal equilibrium is achieved through the constant interactions among electrons, ions, and neutral particles. Examples of thermal equilibrium plasma include natural fusion reactors like the Sun, magnetically confined plasmas in tokamaks, and inertially confined plasmas achieved through laser fusion.

(1.7.2.2) Plasma that Non-thermal Equilibrium

In a non-thermal equilibrium plasma, momentum transfer between light electrons and heavier particles such as ions and neutrals is not nearly as effective. Consequently, the electrons absorb the majority of the energy introduced into the plasma, resulting in a significantly higher electron temperature (T_e) than that of ions (T_i) and neutrals (T_n). Nonthermal equilibrium plasmas can be generated through a variety of methods, including corona discharge, glow discharge, arc discharge, capacitively coupled discharge, inductively coupled discharge, and wave-heated plasma. The applications of these plasmas are diverse, encompassing aerospace, biomedicine, textile technology, environmental engineering, and analytical chemistry.

(1.7.2.3) Plasma That Local Thermal Equilibrium

The local thermal equilibrium plasma is distinct from both thermal equilibrium plasma and nonthermal equilibrium plasma. The electrons, positive ions, and neutral particles are approximately at the same temperature in a state of near equilibrium, which is referred to as local thermal equilibrium ($T_e \approx T_i \approx T_n$).

Local thermal equilibrium (LTE) plasma is characterized by high ion temperatures, reaching 3,000–10,000 K (0.4–1 eV). However, their electron temperatures remain relatively low (0.4–1 eV) in comparison to nonthermal plasmas. A variety of methods, including DC and RF arcs and induction torches, can produce plasmas in regions in thermal equilibrium. These plasmas have many applications, including: Plasma Spray: Used to coat surfaces. .

(1.7.2.4) the non-equilibrium plasma (Non-thermal plasma)

Cold plasma is a type of plasma where most of the electrical energy is directed towards energizing the electrons instead of heating the entire gas. When electrons gain high energy in a plasma, they become very energetic, whereas the ions and neutral particles remain at or near room temperature. This results in the

electron temperature (Te) being significantly higher than the temperatures of the ions and gas ($T_i \approx T_g$). Generally, these temperatures fall within the range of 0.03 to 0.1 electron volts (eV) [26].

Non-thermal plasmas can be generated by devices such as glow discharge, corona discharge, air pressure plasma jet (APPJ), dielectric barrier discharge (DBD), and plasma needles. These cold plasmas are appropriate for low-temperature chemical processes and can be employed to address heat-sensitive materials, such as polymers and biological tissues, due to the fact that the ions and neutral particles remains relatively chilly. Cold plasma possesses a variety of advantageous attributes, including the ability to operate at low gas temperatures, generate reactive chemical species, and exhibit high selectivity. Additionally, it maintains a robust thermodynamic non-equilibrium state. These characteristics increase the potential for the use of cold plasma in a wide variety of applications [32].

Cold plasma technology is essential for the development of sophisticated microelectronics and materials. Its advantages, notably at low temperatures, are currently being examined in a variety of disciplines. The objective of employing low-temperature plasma techniques is to regulate the production of free radicals, electrons, and ions on a surface. This regulation permits the modification of surface properties by either adding or removing material, as demonstrated by processes such as sputtering or etching [26].

(1.8) Plasma Applications

The technical foundation of a variety of applications, such as medicine, biomedical technology, electronics, space physics, illumination, gas lasers, and solid-state plasma, is plasma. Its applications are diverse and include nanotechnology, prostate cancer treatments, semiconductor processing, copper bonding, plasma polymerization, surface treatments, antenna beam formation, plasma display panels, plasma torches, and plasma source ion implantation.

Plasma technology is also essential for the neutralization of radioactive waste, plasma cutting, and pollution control. The significance of plasma technology in the medical field is swiftly expanding, resulting in a decrease in the cost of production and control apparatus [33].

(1.8.1) Applications of Plasma Liquid Systems

The reduction of metal ions in solution is the process by which nanoparticles are synthesized, resulting in a variety of particle sizes, shapes, and constituents. Wet chemical techniques are effective; however, they require several hours to complete. Researchers are exploring alternative methods using energetic electrons as reducing agents to address this lengthy processing time [34]. Plasma interaction with liquids is significant due to their unique characteristics and metal ion dissolved capacity. In cold or non-equilibrium plasmas, free electrons can reach high temperatures, triggering ionization and chemical reactions, while ions and molecules remain at their original temperatures [35]. The plasma-liquid interface method for nanoparticles synthesis offers a simple experimental setup, continuous production during plasma exposure, and eliminates the need for reducing agents [36]. Plasma-liquid interfaces (PLIs) are essential for the synthesis of nanomaterials, as they enable the direct generation of reduction agents, which is a substantial advantage over conventional wet-chemical solutions. Physical and chemical interactions at the plasma-liquid interface, such as sputtering, reduction, and oxidation, influence the formation of nanoparticles. Shira Fuji's research used numerical modeling to show that fluid ions remain in contact with plasma at the fluid's surface when subjected to an AC-driven dielectric barrier discharge. Ions moving slowly in the liquid interact with gas-phase plasma species, influencing reactions and final product formation in the liquid phase. Plasma-based nanomaterials have been proven effective in treatment applications, but synthesis remains challenging due to complex interactions and high voltage discharges. Controlling synthesis rate

and nanoparticle morphology is also challenging, and studying interfacial plasma properties presents challenges [37, 38]. Ionic liquids are suggested as ideal candidates for plasma-assisted nanoparticle synthesis due to their unique properties like low vapor pressure, high heat capacity, and non-flammability. They can be used in plasma vacuum systems and low-pressure plasma environments, improving efficiency and output in nanomaterial synthesis [39]. Ionic liquids can be challenging to modify the surface properties of nanoparticles (NPs), as they have lower solubility compared to water. Additionally, many mineral salts have lower solubility in ionic liquids. Plasma-induced reduction is generally more effective in water due to its more fluid particles [34]. Research on nanoparticle fabrication using water plasma systems, including DC discharges, pulsed DC discharges [40], DC arc discharges [41], and atmospheric microplasmas [41], has shown that the composition of nanoparticles varies between aqueous and air environments [42]. Studies have found that particles generated in water are smaller than those produced in air.

(1.9) Literature Review

Robert Redusz et al. (2014) this paper presents and discusses the most current discoveries in the field of copper oxide thin film gas sensors. For commercial applications, several processes and deposition techniques are shown, together with their benefits and drawbacks. CuO thin film gas sensors have recently been examined for detecting a number of substances in a variety of applications, including agriculture, including nitrogen oxides, carbon oxides, hydrogen sulfide, ammonia, and a variety of volatile organic compounds. CuO thin film gas sensors had outstanding 3-S characteristics (sensitivity, selectivity, and stability). It has also been proven that the material can function at room temperature while preserving long-term stability, making it ideal for gas-sensing applications such as exhaled breath analysis [43].

Y.H. Navale et al. In (2017) successfully fabricated CuO films on a quartz substrate using a simple and catalyst-free thermal evaporation process. The chemical resistance capabilities of the copper oxide (CuO) films toward several target gases were studied. Structural investigation showed that single-phase polycrystalline CuO was formed. Morphological analysis revealed that CuO formed a nanoscale surface morphology. According to the gas sensing data, the CuO films made of nanocubes (NCs) exhibit fast response and recovery times and a high degree of selectivity toward nitrogen dioxide (NO_2) oxidation when compared with other target gases. The maximum response value of CuO sensor sheets at 150 °C is between 76% and 100 ppm of NO_2. Moreover, NO_2 gas can be detected by CuO films at concentrations as low as 1 ppm. The effect of operating temperature on CuO film NO_2 sensing capabilities has been the subject of numerous investigations and reports. Impedance spectroscopy was used to examine the mechanism of interaction between the NO_2 gas molecules and the CuO sensor layer [44].

Artur Rydosz In (2018), investigated current advances in thin-film copper-oxide sensors for gases. His study investigated numerous deposition processes, emphasizing both benefits and drawbacks for commercial application. CuO thin-film detectors were investigated for detecting a variety of chemicals, including nitrogen oxides, carbon oxides, hydrogen sulfide, ammonia, and different volatile organic compounds, spanning a wide range of applications. The sensors themselves display amazing effectiveness relation to sensitivities, selection, and reliability. Furthermore, nanomaterials demonstrated longevity at ambient temperature, making them ideal for gas sensing activities like evaluating breathing air [45].

Hooch Antink et al. In 2018, a copper-silver oxide composite electrode was fabricated using a precursor ink. A copper-silver oxide barrier had been produced using the hybrid dye that dissolved entirely at 150 °C in ambient air and comprised both silver and copper predecessors. The addition of copper precursors increased the silver ink's electrocatalytic efficiency in reducing hydrogen peroxide (H_2O_2). The manufactured electrodes were used to create an amperometric sensor with a linear response across a wide range and a low detection limit of 4.0 μM (S/N = 3). In addition, the sensor displayed outstanding stability, repeatability, and anti-interference properties [46].

Dinesh and Kumar In 2019, The study looked into the production of copper oxide and silver-doped copper oxide nanostructures using Muntingia calabura leaf extract. The researchers examined the antibacterial characteristics associated with these nanostructures. Researchers showed a leaf extract was helpful in decreasing and stabilizing tiny particles, resulting in improved properties such as increased ultraviolet absorbance and visible light absorbance. Furthermore, the research they conducted demonstrated a novel eco-friendly synthesis process

based on Mcalabura leaf extract, revealing the antibacterial abilities of Ag-doped CuO nanoparticles [47].

S. B. Tharchanaa et al. In (2020), Nanomaterials were manufactured from industrial waste in an environmentally acceptable manner. Copper and copper oxide nanoparticles were effectively produced from copper scrap using the plasma arc discharge method in N2 and air conditions. The nanoparticles were confirmed by X-ray diffraction, UV-visible spectrometry, and energy dispersive spectrometry. A high-resolution transmission electron microscopy study was conducted to analyze the shape and average particle size of nanoparticles that were generated. The findings revealed that the small particles have a spherical and deformed form, with typical size of particles of 78 nm and 67 nm to and cuo, according [49].

A.A. Menazeaa and S. Awwad In (2020), Using pulsed laser deposition (PLD), we created a thin coating of silver/copper oxide nanocomposite. They used a subsequent generations millisecond fundamental optical with an emission wavelength of 532 nm for the beam of light source. A sliver/copper oxide composite film was created to act as a catalytic sheet in decreasing the amount of the nitrophenol.

This composite thin film were examined using a variety of analytical methodologies. The effective crystallization of both the CuO thin films and the Ag/CuO nanocomposite thin films was confirmed by XRD. Furthermore, UV-visible spectroscopy demonstrated that the Ag/CuO nanoporous thin film exhibited superior transmittance values in comparison to the CuO thin film. The direct energy bandgap of CuO thin films was determined to be 2.51 eV. Nevertheless, this value decreased to 2.15 eV in the Ag/CuO nanostructured thin films. The copper oxide nanoparticles were predominantly spherical, as indicated by the FE-SEM analysis.

With some silver nanoparticles also observed dispersed within them. The Ag/CuO nanocomposite thin films demonstrated enhanced catalytic activity, reducing the time required for 4-nitrophenol reduction from 90 minutes to 30 minutes [50].

K. Dyndał, et al. In (2020) produced ultra-thin copper oxide (CuO) films by sputtering a copper target in pure argon. Using magnetron sputtering technology with the glancing angle deposition method (GLAD) in a reactive mode, adjusted the material's tilt between 45 to 85 and 0 degrees, but additionally maintaining the specimen spinning at an average of 20 rotations each minute. The films had been heated in the air at 400°C for four hours after deposition. The methods of XRD, EDX, X-ray reflectance (XRR), and optical spectroscopy have been utilized to study the composition, shape, and optical properties of ultra-thin CuO films. Various profilometer has been employed to determine the thicknesses of the motion pictures after they had been created. Copper oxide formations have been examined as polymers are susceptible to gas attack after being exposed towards solvent at a concentration of less than ppm.Following deposition, gas-sensing values were calculated at 300, 350, and 400 oC and 50% (RH). Researchers observed this device's responsiveness rises as the amount of CuO light coatings rises, using the best findings obtained with an object that was 8 nm thin [51].

H.M. Mahesh, et al. In (2021), the researchers created copper oxide particles by oxidizing copper (Cu) or cuprous oxide, which were previously made by chemically reducing Cu^{+2} ions using ascorbic acid. The specimen includes CuO, as shown through an XRD examination. In addition, FE-SEM scans showed the particles had been packed together with sizes varying from 25 to 30 nanometers. The wavelength-dependent absorption spectra revealed a band gap energy of 3.7 eV, far greater than the value for ordinary CuO.

In addition, the Néel the temperature, which marks the shift from ferromagnetic to antiferromagnetic conduct had been present 230 K. Magnetism loops of hysteresis obtained at 5 K showed poor magnetic characteristics. Direct current (DC) electrical conductivity studies were done at temperatures ranging from 300 to 500 K, yielding an activation energy of 0.36 eV. The gas sensing abilities of CuO for NO_2 showed exceptionally successful within the internal temperature range of 200 to 300°C, in sensitivity improving as gas concentrations raised. However, temperature had little effect on outcomes [52].

Researchers S. B. Tharchanaa et al. In (2021), Produce Cu and CuO NPs via the plasmonic process, used cu with an initial matter. For properties NPs, it studies various analysis process are XRD, UV-Vis spectrum, and EDS spectroscopy. Furthermore, transmission electron microscopy with high resolution was employed to investigate the shape of particles and sizes. The particles had been evaluated for bactericidal operations that exhibited strong inhibition against gram-negative as well as gram-positive bacteria. The biggest inhibitory regions have been detected for the species staphylococcus aureus and klebsiella pneumoniae were situated at 32 mm and 28 mm, significantly [53].

By Navale, Y.H. et al. In (2021) CuO/ZnO heterostructures that are were created using a catalyst-free thermal evaporation process and subsequently annealed in either argon gas or air. Prior to the sensing measurements, the heterostructures that are' structure, morphology, and composition were investigated using XRD, EDS, and SEM techniques. Gas sensing studies suggest that thermally evaporated CuO/ZnO heterostructures may effectively detect NO_2 at degrees as low as 150 °C. These CuO/ZnO hybrid structures demonstrated good gas response stability and reversibility, reaching a maximum response of 96% at 100 ppm NO2. The primary purpose of this study is to investigate how NO_2 gas reacts using

CuO/ZnO this heterojunction sensing substances, that could help in recognizing of NO_2 [55].

A study conducted by Zhakypov et al., in (2023) a unique approach for producing copper oxide nanoparticles has been introduced. The study participants used a regulated, one-step technique employing arc discharge in deionized water, which eliminated the requirement for thermal annealing. The arc discharge current was varied between 2 and 4 A to adjust the experimental parameters. To analyze the synthesized nanoparticles, technologies such as X-ray diffraction, Raman spectroscopy, and power dispersive analysis consisted used. Those techniques revealed information about the crystalline structure and basic makeup inside the nanocrystals. This turned out that raising the arc current of discharge caused a higher copper-to-oxygen ratios as smaller particle sizes. The combination approach permits for the control of the outcome material's band gap with modifying the copper oxide ratio, nanoparticle shape, and crystallite size [56].

(Min Kim), et al. In (2023) presented a straightforward and scalable synthesis technique to create silver-functionalized porous ZnO sheets, along with an enhanced set of properties for NO_2 gas detection. Using a one-pot synthesis technique based on the hydrothermal process, functionalised porous ZnO sheets with well-dispersed submicron silver particles were created from zinc and silver precursors. The gas sensor composed of 3% silver-functionalized porous ZnO sheets was shown to have increased NO_2 gas sensing performance (response, selectivity, response time, and recovery time) at 200 °C. Because of the combined effects of increased resistance from the formation of a Schottky barrier at the silver-zinc junctions and enhanced NO_2 gas adsorption in the presence of silver particles, we were able to demonstrate a response (Rg/Ra) ranging from 17.18 to 10 ppm of NO_2 gas and obtain a high response of 14.05 even at 60% relative humidity [57].

S. M. Ingole In (2023), fabricated a CuO nanoparticle sensor film on a glass substrate using catalyst-free thermal evaporation of Cu powder and air annealing at 700 °C. Further characterization was carried out using XRD, SEM, and EDAX analysis to confirm its structure, morphology, and composition. The chemical gas sensing capabilities of CuO nanoparticles toward various oxidizing and reducing gases were investigated. In contrast to other test gases, the experimental results showed that CuO nanoparticles were highly sensitive and selective toward NO_2gas. At an optimum temperature of 1500 °C, CuO nanoparticles responded to NO_2 gas with a maximum of 29% at a concentration of 100 ppm and with a very fast reaction time [58].

Bahaa Abbas et al. In 2024 Argon plasma jets were employed for preparing cuo nanocrystals. To characterize the prepared copper oxide nanoparticles, various techniques were used, including UV-Vis spectroscopy, x-ray diffraction (XRD), x-ray energy dispersive spectroscopy (EDS), and filed emission-scanning electron microscopy. Ultraviolet (UV)-visible spectroscopy found that the cuo nanoparticles had an energy band gap of 2.7 eV. A method called X-ray diffraction evaluation revealed that the cuo nps had a norm crystallographic amount of 36 nm.

In addition, an EDX test results showed the formation of very pure cuo nps. The outside topology was investigated via the technique of scanning electron microscopy, resulting demonstrated an important level of amplification. Due to the SEM research, the nanoparticles of copper oxide had an average diameter of 10 nm. [59].

1.13 Aim of the Work

In this study, we synthesized silver nanoparticles and copper oxide nanoparticles using Plasma Jet technology, combined these materials to form a composite, and analyzed their properties both before and after the combination. We investigated various aspects of their structure, optical behavior, electrical Characteristics, and sensory properties. To achieve this, we employed a range of techniques including X-ray diffraction (XRD), field emission scanning electron microscopy (FESEM), UV-VIS spectroscopy, Fourier transform infrared spectroscopy (FTIR), and energy dispersive X-ray (EDX) analysis. Additionally, we examined the gas-sensing capabilities of the copper oxide and silver nanomaterials, as well as the CuO-Ag composites, specifically focusing on their response to different concentrations of NO2 gas.

الخلاصة

في هذا العمل، تم تصنيع جسيمات نانوية من أكسيد النحاس النقي (CuO NPs) وجسيمات نانوية من الفضة النقية (Ag NPs) ومتراكبات أكسيد النحاس مع الفضة (CuO/Ag NPs) بنسب وزنية مختلفة (٠، ١، ٣، ٦، ٩ و١٢٪ وزنيًا) بنجاح باستخدام تقنية تحضير نفث البلازما. تُعرف تقنية نفث البلازما بأنها تقنية منخفضة التكلفة وبسيطة وغير سامة تُستخدم في تصنيع جسيمات نانوية من أكسيد النحاس النقية وعالية التبلور وجسيمات نانوية من الفضة وجسيمات نانوية من أكسيد النحاس/الفضة. تم التحقيق في الخصائص البنيوية (XRD, EDX, FESEM و FT-IR) والخصائص البصرية وأداء استشعار الغاز لعينات جسيمات نانوية من أكسيد النحاس وجسيمات نانوية من الفضة المصنعة، ودراسة تأثير نسبة التشويب على خصائص الأغشية الرقيقة لجسيمات نانوية من أكسيد النحاس.

أظهرت نتائج مجهر مسح الانبعاث الإلكتروني الميداني (FESEM) وحيود الأشعة السينية (XRD) الحصول على بنية جسيمات نانوية مكعبية نقية عالية التبلور من أكسيد النحاس مع شكل شبه كروي يشبه الشكل وبنية جسيمات نانوية أحادية الميل من الفضة مع جسيمات نانوية كروية موحدة تشبه شكل الفضة، وكان متوسط أحجام الجسيمات (٥٠ نانومتر) و (٣٨ نانومتر) على التوالي. أثبت EDX و FTIR التركيب الكيميائي والمجموعات الوظيفية والتفاعلات الجيدة بين جسيمات النانو من النحاس وجسيمات النانو من الفضة كمواد مضافة داخل أغشية النانو المركبة من أكسيد النحاس/الفضة. تم التحقيق في أطياف الامتصاص والنفاذية ضمن نطاق الطول الموجي (٣٠٠ - ١١٠٠ نانومتر)، وكشفت النتائج أن محلول أكسيد النحاس النقي سجل قدرة امتصاص أعلى عند طول موجي محدد، وأدى إضافة جسيمات النانو من الفضة إلى تقليل قدرة الامتصاص، بينما أظهرت النفاذية علاقة عكسية مع الطول الموجي. بالإضافة إلى ذلك، تعتمد قيم الامتصاص والنفاذية بشكل كبير على محتوى جسيمات النانو الفضية وطول الموجة، حيث لوحظ أن إضافة محتوى مختلف من جسيمات النانو الفضية إلى محلول جسيمات النانو النحاسية النقية أدى إلى انخفاض في النفاذية وزيادة في الامتصاص. من ناحية أخرى، أظهرت نتائج الانعكاس أن زيادة الطول الموجي تسبب في انخفاض في قيم الانعكاس نتيجة لانخفاض معامل الانكسار مع طول الموجة بسبب جسيمات النانو الفضية المضافة، حقق محلول جسيمات النانو النحاسية النقية أقصى قيم الانعكاس. أظهر معامل الامتصاص لمحلول جسيمات النانو النحاسية النقية ذروة عالية في نطاق الطاقة (٣ - ٣,٥ إلكترون فولت) كدالة لطاقة الفوتون، عند زيادة جسيمات النانو الفضية داخل بنية محلول أكسيد النحاس لوحظ انخفاض كبير في قيمة معامل الامتصاص.

تم حساب فجوات نطاق الطاقة للمحاليل المُحضرة. أظهرت المحاليل الناتجة فجوة نطاق طاقة مباشرة. وتبين ان فجوة نطاق الطاقة تقل عند النسب القليلة جسيمات النانو الفضية لكنها تزداد عندما تكون النسب

عالية، ويُحتمل أن تؤدي إضافة جسيمات النانو الفضية إلى تغير فجوة الطاقة نظرًا لارتفاع حالات الشوائب التي تؤثر على بنية فجوة النطاق. أظهر محلول جسيمات النانو من أكسيد النحاس المُشَبَّبة بنسبة (٠,٠١) أقل قيمة لفجوة نطاق الطاقة (٢,٥١٣ إلكترون فولت)، بينما اعلى قيمة لفجوة الطاقة عند النسبة (٠,١٢) وتساوي (٣,١٨٥ إلكترون فولت). وان الانتقالات الإلكترونية للأغشية المُحضرة مباشرة.

أظهرت النتائج أيضًا أن معامل الانكسار ومعامل الخمود للعينات النقية والمحضرة ينخفضان مع زيادة طاقة الفوتون. زاد ثابت العزل الحقيقي بإضافة محتوى متغير من جسيمات النانو الفضية إلى جسيمات النانو النحاسية النقية، بينما انخفض ثابت العزل التخيلي خطيًا مع طاقة الفوتون الساقط للمواد النقية، ولكن عند إضافة جسيمات النانو الفضية تغير معدل الارتفاع.

أظهرت خصائص مستشعر الغاز أن المقاومة الكهربائية (R_a) لجميع مستشعرات الأغشية الرقيقة مستقرة في الهواء. ولكن عندما تم اختبار مستشعرات الأغشية الرقيقة تحت غاز NO_2 (٥٠٠ جزء في المليون)، زادت المقاومة الكهربائية (R_g) لمستشعر (A) كدالة لوقت التعرض، وانخفضت (R_g) لمستشعرات (B إلى G) في حالة الغاز المفتوحة، بينما انخفضت بالنسبة لمستشعر (A) ثم ارتفعت بسرعة في حالة الغاز المغلقة. أظهرت جميع المستشعرات المحضرة سلوكًا من النوع n عند تطبيق غاز NO_2، وانخفضت الموصلية الكهربائية للمستشعرات وزادت المقاومة الكهربائية. وجود غاز NO_2في جميع المستشعرات المصنوعة من سلوك النوع n، حدث سلوك معاكس عند تطبيق NO_2على مستشعرات الأغشية الرقيقة ذات السلوك P B-G.

سجلت حساسية (S %) لغاز NO_2 للمستشعرات المحضرة قيمًا مختلفة كدالة لدرجة الحرارة ومحتوى المتراكبات. بشكل عام، سجلت جميع المستشعرات حساسية جيدة (S%) عند درجات حرارة معتدلة (٥٠ و١٠٠ و١٥٠ درجة مئوية) وحساسية منخفضة عند درجات حرارة عالية (٢٠٠ درجة مئوية)، في حين أدى إضافة جسيمات النانو الفضية إلى زيادة كبيرة في قيم الحساسية، وعلى العكس من ذلك، في حالة الغاز المغلق، تزداد مقاومة جميع المستشعرات عند التعرض لثاني أكسيد النيتروجين ($R_{gas} > R_{air}$)، مما أدى إلى انخفاض الحساسية (S%).

جمهورية العراق

وزارة التعليم العالي والبحث العلمي

جامعة ديالى - كلية العلوم -قسم الفيزياء

تحضير وتوصيف المتراكبات النانوية (CuO-Ag) باستعمال طريقة نفاث البلازما كمتحسس غازي

اطروحة مقدمة إلى

مجلس كلية العلوم - جامعة ديالى

وهي جزء من متطلبات نيل درجة الماجستير

في علوم الفيزياء

من قبل

شيماء فاضل محمد

بكالوريوس في الفيزياء – جامعة بغداد (٢٠٠٢)

اشراف

ا.م.د ألفت أحمد محمود ***ا.م.د.دينة علي لطيف***

2025 A.D. **1446 A.H.**